Acta Mech 226:475–490 (2015)
DOI 10.1007/s00707-014-1193-2

Jeng-Tzong Chen · Jia-Wei Lee · Yi-Chuan Kao · Shyue-Yuh Leu

Eigenanalysis for a confocal prolate spheroidal resonator using the null-field BIEM in conjunction with degenerate kernels

Received: 24 March 2014 / Revised: 26 May 2014 / Published online: 21 July 2014
© Springer-Verlag Wien 2014

Abstract In this paper, we employ the null-field boundary integral equation method (BIEM) in conjunction with degenerate kernels to solve eigenproblems of the prolate spheroidal resonators. To detect the spurious eigenvalues and the corresponding occurring mechanisms which are common issues while utilizing the boundary element method or the BIEM, we use angular prolate spheroidal wave functions and triangular functions to expand boundary densities. In this way, the boundary integral of a prolate spheroidal surface is exactly determined, and eigenequations are analytically derived. It is revealed that the spurious eigenvalues depend on the integral, representations and the shape of the inner boundary. Furthermore, it is interesting to find that some roots of the confocal prolate spheroidal resonator are double roots no matter that they are true or spurious eigenvalues. Illustrative examples include confocal prolate spheroidal resonators of various boundary conditions. To validate these findings and accuracy of the present approach, the commercial finite-element software ABAQUS is also applied to perform acoustic analyses. Good agreement is obtained between the acoustic results obtained by the null-field BIEM and those provided by the commercial finite-element software ABAQUS.

1 Introduction

Eigenanalysis is a fundamental issue for vibration, acoustics and electromagnetic wave propagation such as loudspeaker enclosures, fluid-filled vessels, muffler systems, vehicle compartments, aircraft cabins and waveguides. It is a useful reference for safety and comfort designs. Besides, it also can provide a base for the structural health monitoring in recent years. To offer resonance frequencies and modes obtained by model tests or numerical analyses is very important. From the view point of cost, numerical analyses are more efficient than model tests. Therefore, a demand for eigenanalysis is to develop an efficient and reliable method for computations of eigenvalues and eigenmodes. During the recent decades, many numerical methods have been employed to solve eigenproblems. Two approaches, the finite element method (FEM) and the boundary element method (BEM), have been recognized as effective methods in numerical analyses. Although the FEM is a popular method for solving eigenproblems, it needs a lot of time to generate the mesh for problems with complex geometries. In this aspect, the BEM is an efficient alternative from the viewpoint of mesh reduction.

J.-T. Chen · J.-W. Lee · Y.-C. Kao
Department of Harbor and River Engineering, National Taiwan Ocean University, Keelung, Taiwan

J.-T. Chen (✉)
Department of Mechanical and Mechatronic Engineering, National Taiwan Ocean University, Keelung, Taiwan
E-mail: jtchen@mail.ntou.edu.tw
Tel.:+886-2-24622192

S.-Y. Leu
Department of Aviation Mechanical Engineering, China University of Science and Technology, Hsinchu, Taiwan

For 2D eigenproblems, Tai and Shaw [1] first employed the complex-valued BEM to solve membrane vibration. De Mey [2] revisited this problem in 1976. Later, De Mey [3] proposed a simplified approach by using only the real part or imaginary part kernel where he found that spurious solutions were imbedded as well as the ill-conditioned matrix appeared. In a similar way of using the real part kernel, Hutchinson [4,5] solved the free vibration of a plate. Also, Yasko [6] as well as Duran et al. [7] employed the real part kernel approach. Chen and his NTOU/MSV group proposed the null-field BIEM in conjunction with degenerate kernels to solve eigenproblems containing circular [8] or elliptical holes [9]. The advantage of being free of calculating the principal value is gained. Their approach is a semi-analytical method since errors only occur from the truncation of the number of the boundary density.

Regarding 3D eigenproblems, Tsai et al. [10] used the method of fundamental solutions to determine the eigenvalues of a concentric sphere. Chen et al. [11] also considered the same problem by using the null-field BIEM. Chang [12] determined the natural frequencies of a prolate acoustical resonator. Chen [13] employed the variational formulation to calculate natural frequencies. Both Dirichlet and Neumann boundary conditions were considered. Filippi [14] used the integral equation method to obtain eigenfrequencies of an oblate spheroidal cavity containing a concentric sphere. In 1999, Kokkorakis and Roumeliotis [15] extended the problem considered by Filippi to a prolate spheroidal cavity containing a concentric penetrable sphere by using the wave function expansion and the shape perturbation method.

Although the BEM or BIEM only generates the mesh on the boundary, it may face with the calculation of the principal value and the pollution of spurious eigenvalues. When we deal with the simply connected problems by using only the real or the imaginary part kernel [16,17], spurious eigenvalues may appear. Even though we employ the complex-valued kernel for eigenproblems containing multiply connected domain, the spurious eigensolutions also occur [18,19]. Therefore, it is not trivial to study the appearing mechanism of spurious eigenvalues. Kuo et al. [16] proved the existence of spurious eigensolutions and pointed out that spurious eigenvalues occur at the zeros of the mth-order Bessel functions of the second kind or their derivatives through a circular membrane for the real part dual BEM. Later, Chen et al. [20], and Lee and Chen [21] extended a circular membrane to a circular plate by using the real-part BEM and BIEM, respectively. Later, they also extended studies of circular membranes to elliptical ones [22]. Besides, Shi et al. [23] employed the boundary knot method to solve the problem of free vibration of thin plates. Then, Chen et al. [24] numerically investigated spurious eigenvalues of plate problems by using the non-dimensional dynamic influence function method. For multiply connected eigenproblems, Chen et al. [9,11,18,19] employed the degenerate kernels to analytically study the reason why spurious eigenvalues may occur in the cases of an annular and a confocal ellipse, even though the complex-valued kernels are used. They found that spurious eigenvalues depend on the geometry of inner boundary and the integral representation. Extension to study 3D problems is not trivial.

Following the successful experiences of employing the null-field BIEM to solve eigenproblems containing circular and elliptical boundaries, respectively, we extend the null-field BIEM to analytically study the eigenproblems of the confocal prolate spheroidal resonator in this paper. A null-field BIEM is utilized in conjunction with the degenerate kernel and the eigenfunction expansion. To fully utilize the prolate spheroidal geometry for an analytical study, the prolate spheroidal coordinates and prolate spheroidal wave functions [25,26] are used. To describe the discontinuity of double-layer potential, three alternatives were provided. One is the Taylor expansion with respect to the boundary density function. Another is the bump contour with respect to the boundary contour integral. The other is to express the closed-form fundamental solution into the expression of the degenerate kernel. Here, the last technique is considered. The fundamental solution is expanded to the degenerate kernel [27] in the prolate spheroidal coordinates. Also, the boundary densities are expanded by using the eigenfunction expansions. The advantage of being free of calculating the principal value is also gained. Finally, the true and spurious eigenequations of the confocal prolate spheroidal resonator are analytically derived by using the null-field BIEM and numerically verified by using the commercial finite-element software ABAQUS.

2 System of prolate spheroidal coordinate and problem statement

2.1 System of prolate spheroidal coordinate

For the prolate spheroidal coordinates, the relation of (ξ, η, ϕ) to the 3D Cartesian coordinates. (x, y, z) is defined as

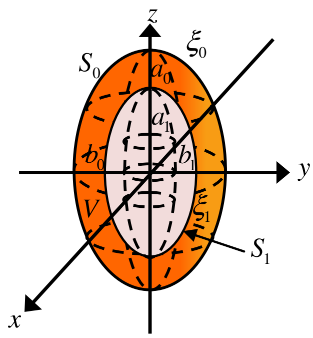

Fig. 1 Sketch of a confocal prolate spheroidal resonator

$$\begin{cases} x = c\sqrt{(\xi^2-1)(1-\eta^2)}\cos(\phi), \\ y = c\sqrt{(\xi^2-1)(1-\eta^2)}\sin(\phi), \\ z = c\xi\eta, \end{cases} \tag{1}$$

where c is the semi-focal length and the range of the three coordinates is

$$1 \leq \xi, -1 \leq \eta \leq 1, 0 \leq \phi \leq 2\pi. \tag{2}$$

2.2 Problem statement

For the eigenproblem of a confocal prolate spheroidal resonator as shown in Fig. 1, the acoustic pressure satisfies the Helmholtz equation as follows:

$$(\nabla^2 + k^2)u(\mathbf{x}) = 0, \quad \mathbf{x} \in V \tag{3}$$

where ∇^2 is the Laplacian operator, k is the wave number, $u(\mathbf{x})$ is the acoustic pressure, $\mathbf{x}$ is the field point and V is the domain of interest. As shown in Fig. 1, a_0 and b_0 are the lengths of semi-major and semi-minor axes for the outer prolate spheroid, a_1 and b_1 are the lengths of semi-major and semi-minor axes for the inner prolate spheroid, ξ_0 and ξ_1 stand for the radial coordinates for the outer and inner prolate spheroids, respectively, S_0 and S_1 stand for the surfaces for the outer and inner prolate spheroids, respectively. For this confocal case, the analytical solution can be derived in the prolate spheroidal coordinates since we can utilize global prolate spheroidal coordinates to describe the inner and outer surfaces simultaneously as shown later.

3 Dual boundary element formulations—the conventional version

Based on Green's third identity, the dual boundary integral equations for the boundary point are shown below:

$$2\pi u(\mathbf{x}) = C.P.V. \int_S T^c(\mathbf{s},\mathbf{x})u(\mathbf{s})dS(\mathbf{s}) - R.P.V. \int_S U^c(\mathbf{s},\mathbf{x})t(\mathbf{s})dS(\mathbf{s}), \ \mathbf{x} \in S, \tag{4}$$

$$2\pi t(\mathbf{x}) = H.P.V. \int_S M^c(\mathbf{s},\mathbf{x})u(\mathbf{s})dS(\mathbf{s}) - C.P.V. \int_S L^c(\mathbf{s},\mathbf{x})t(\mathbf{s})dS(\mathbf{s}), \ \mathbf{x} \in S \tag{5}$$

where Eqs. (4) and (5) are singular and hypersingular boundary integral equations, respectively, $R.P.V.$, $C.P.V.$ and $H.P.V.$ denote the Riemann principal value (Riemann sum), Cauchy principal value and Hadamard (or the so-called Mangler) principal value, respectively, $t(\mathbf{x}) = \partial u(\mathbf{x})/\partial n_{\mathbf{x}}$, $\mathbf{s}$ is the position vector of the source point of the fundamental solution, S is the surface of the object, and $U^c(\mathbf{s}, \ \mathbf{x})$ is the closed-form fundamental solution which satisfies

$$(\nabla^2 + k^2)U^c(\mathbf{s},\mathbf{x}) = 4\pi\,\delta(\mathbf{x}-\mathbf{s}), \tag{6}$$

where the closed-form fundamental solution is

$$U^c(\mathbf{s},\mathbf{x}) = -\frac{e^{ikr}}{r} = -ikh_0^{(1)}(kr), \tag{7}$$

in which $r \equiv |\mathbf{s}-\mathbf{x}|$ is the distance between the source point and the field point, and $h_0^{(1)}(kr)$ is the *zero*th-order spherical Hankel function of the first kind. The other closed-form kernel functions, $T^c(\mathbf{s},\mathbf{x})$, $L^c(\mathbf{s},\mathbf{x})$ and $M^c(\mathbf{s},\mathbf{x})$ are defined by

$$T^c(\mathbf{s},\mathbf{x}) = \frac{\partial U^c(\mathbf{s},\mathbf{x})}{\partial n_{\mathbf{s}}}, \tag{8}$$

$$L^c(\mathbf{s},\mathbf{x}) = \frac{\partial U^c(\mathbf{s},\mathbf{x})}{\partial n_{\mathbf{x}}}, \tag{9}$$

$$M^c(\mathbf{s},\mathbf{x}) = \frac{\partial^2 U^c(\mathbf{s},\mathbf{x})}{\partial n_{\mathbf{s}}\partial n_{\mathbf{x}}}. \tag{10}$$

3.1 Dual null-field boundary integral formulations—the present version

By introducing degenerate kernels to represent the closed-form fundamental solution, the collocation point can be exactly located on the real boundary without the need of calculating the principal value in the bump contour approach. By choosing the proper degenerate kernels, the representations of the conventional integral equations including the boundary point can be written as

$$4\pi u(\mathbf{x}) = \int_S T^d(\mathbf{s},\mathbf{x})u(\mathbf{s})dS(\mathbf{s}) - \int_S U^d(\mathbf{s},\mathbf{x})t(\mathbf{s})dS(\mathbf{s}),\ \ \mathbf{x}\in V\cup S, \tag{11}$$

$$4\pi t(\mathbf{x}) = \int_S M^d(\mathbf{s},\mathbf{x})u(\mathbf{s})dS(\mathbf{s}) - \int_S L^d(\mathbf{s},\mathbf{x})t(\mathbf{s})dS(\mathbf{s}),\ \ \mathbf{x}\in V\cup S, \tag{12}$$

and

$$0 = \int_S T^d(\mathbf{s},\mathbf{x})u(\mathbf{s})dS(\mathbf{s}) - \int_S U^d(\mathbf{s},\mathbf{x})t(\mathbf{s})dS(\mathbf{s}),\ \ \mathbf{x}\in V^c\cup S, \tag{13}$$

$$0 = \int_S M^d(\mathbf{s},\mathbf{x})u(\mathbf{s})dS(\mathbf{s}) - \int_S L^d(\mathbf{s},\mathbf{x})t(\mathbf{s})dS(\mathbf{s}),\ \ \mathbf{x}\in V^c\cup S \tag{14}$$

where V^c is the complementary domain. It is noted that the observation point of Eqs. (11)–(14) can contain the boundary point ($\mathbf{x}\to B$) since the kernel functions (U^d, T^d, L^d and M^d) are expressed in terms of proper degenerate kernels which will be elaborated later on. Although the symbols for four kernels in Eqs. (11), (12) and (13), (14) are the same, their representation formulae are different. Based on the property of separation variables in the prolate spheroidal coordinates, the closed-form fundamental solution $U^c(\mathbf{s},\mathbf{x})$, other closed-form kernel functions of $T^c(\mathbf{s},\mathbf{x})$ $L^c(\mathbf{s},\mathbf{x})$ and $M^c(\mathbf{s},\mathbf{x})$ can be expressed in terms of the degenerate kernel as shown below:

$$U^d(\mathbf{s},\mathbf{x}) = \begin{cases} U^E(\mathbf{s},\mathbf{x}) = \lim\limits_{N\to\infty} U_N^E(\mathbf{s},\mathbf{x}), & \xi_{\mathbf{x}} \geq \xi_{\mathbf{s}}, \\ U^I(\mathbf{s},\mathbf{x}) = \lim\limits_{N\to\infty} U_N^I(\mathbf{s},\mathbf{x}), & \xi_{\mathbf{x}} < \xi_{\mathbf{s}}, \end{cases} \tag{15}$$

$$T^d(\mathbf{s},\mathbf{x}) = \begin{cases} T^E(\mathbf{s},\mathbf{x}) = \lim\limits_{N\to\infty} T_N^E(\mathbf{s},\mathbf{x}), & \xi_{\mathbf{x}} > \xi_{\mathbf{s}}, \\ T^I(\mathbf{s},\mathbf{x}) = \lim\limits_{N\to\infty} T_N^I(\mathbf{s},\mathbf{x}), & \xi_{\mathbf{x}} < \xi_{\mathbf{s}}, \end{cases} \tag{16}$$

$$L^d(\mathbf{s},\mathbf{x}) = \begin{cases} L^E(\mathbf{s},\mathbf{x}) = \lim\limits_{N\to\infty} L_N^E(\mathbf{s},\mathbf{x}), & \xi_{\mathbf{x}} > \xi_{\mathbf{s}}, \\ L^I(\mathbf{s},\mathbf{x}) = \lim\limits_{N\to\infty} L_N^I(\mathbf{s},\mathbf{x}), & \xi_{\mathbf{x}} < \xi_{\mathbf{s}}, \end{cases} \tag{17}$$

$$M^d(\mathbf{s},\mathbf{x}) = \begin{cases} M^E(\mathbf{s},\mathbf{x}) = \lim\limits_{N\to\infty} M_N^E(\mathbf{s},\mathbf{x}), & \xi_{\mathbf{x}} \geq \xi_{\mathbf{s}}, \\ M^I(\mathbf{s},\mathbf{x}) = \lim\limits_{N\to\infty} M_N^I(\mathbf{s},\mathbf{x}), & \xi_{\mathbf{x}} < \xi_{\mathbf{s}} \end{cases} \tag{18}$$

where $\mathbf{x} = (\xi_{\mathbf{x}}, \eta_{\mathbf{x}}, \phi_{\mathbf{x}})$ and $\mathbf{s} = (\xi_{\mathbf{s}}, \eta_{\mathbf{s}}, \phi_{\mathbf{s}})$ stand for the prolate spheroidal coordinates, $U_N^E(\mathbf{s}, \mathbf{x})$, $U_N^I(\mathbf{s}, \mathbf{x})$, $T_N^E(\mathbf{s}, \mathbf{x})$, $T_N^I(\mathbf{s}, \mathbf{x})$, $L_N^E(\mathbf{s}, \mathbf{x})$, $L_N^I(\mathbf{s}, \mathbf{x})$, $M_N^E(\mathbf{s}, \mathbf{x})$, and $M_N^I(\mathbf{s}, \mathbf{x})$ are degenerate kernels in the prolate spheroidal coordinates (finite-rank approximation) as shown below [27]:

$$U^d(\mathbf{s}, \mathbf{x}) = \begin{cases} U_N^E(\mathbf{s}, \mathbf{x}) = -2ik \displaystyle\sum_{n=0}^{N} \sum_{m=0}^{n} \frac{\varepsilon_m}{\Lambda_{mn}} je_{mn}(q, \xi_{\mathbf{s}}) he_{mn}(q, \xi_{\mathbf{x}}) \\ \qquad S_{mn}(q, \eta_{\mathbf{s}}) S_{mn}(q, \eta_{\mathbf{x}}) \cos[m(\phi_{\mathbf{s}} - \phi_{\mathbf{x}})], \ \xi_{\mathbf{x}} \geq \xi_{\mathbf{s}}, \\ U_N^I(\mathbf{s}, \mathbf{x}) = -2ik \displaystyle\sum_{n=0}^{N} \sum_{m=0}^{n} \frac{\varepsilon_m}{\Lambda_{mn}} je_{mn}(q, \xi_{\mathbf{x}}) he_{mn}(q, \xi_{\mathbf{s}}) \\ \qquad S_{mn}(q, \eta_{\mathbf{s}}) S_{mn}(q, \eta_{\mathbf{x}}) \cos[m(\phi_{\mathbf{s}} - \phi_{\mathbf{x}})], \ \xi_{\mathbf{x}} < \xi_{\mathbf{s}}, \end{cases} \tag{19}$$

$$T^d(\mathbf{s}, \mathbf{x}) = \begin{cases} T_N^E(\mathbf{s}, \mathbf{x}) = -2ik \dfrac{\sqrt{\xi_{\mathbf{s}}^2 - 1}}{c\sqrt{\xi_{\mathbf{s}}^2 - \eta_{\mathbf{s}}^2}} \displaystyle\sum_{n=0}^{N} \sum_{m=0}^{n} \frac{\varepsilon_m}{\Lambda_{mn}} je'_{mn}(q, \xi_{\mathbf{s}}) he_{mn}(q, \xi_{\mathbf{x}}) \\ \qquad S_{mn}(q, \eta_{\mathbf{s}}) S_{mn}(q, \eta_{\mathbf{x}}) \cos[m(\phi_{\mathbf{s}} - \phi_{\mathbf{x}})], \ \xi_{\mathbf{x}} > \xi_{\mathbf{s}}, \\ T_N^I(\mathbf{s}, \mathbf{x}) = -2ik \dfrac{\sqrt{\xi_{\mathbf{s}}^2 - 1}}{c\sqrt{\xi_{\mathbf{s}}^2 - \eta_{\mathbf{s}}^2}} \displaystyle\sum_{n=0}^{N} \sum_{m=0}^{n} \frac{\varepsilon_m}{\Lambda_{mn}} je_{mn}(q, \xi_{\mathbf{x}}) he'_{mn}(q, \xi_{\mathbf{s}}) \\ \qquad S_{mn}(q, \eta_{\mathbf{s}}) S_{mn}(q, \eta_{\mathbf{x}}) \cos[m(\phi_{\mathbf{s}} - \phi_{\mathbf{x}})], \ \xi_{\mathbf{x}} < \xi_{\mathbf{s}}, \end{cases} \tag{20}$$

$$L^d(\mathbf{s}, \mathbf{x}) = \begin{cases} L_N^E(\mathbf{s}, \mathbf{x}) = -2ik \dfrac{\sqrt{\xi_{\mathbf{x}}^2 - 1}}{c\sqrt{\xi_{\mathbf{x}}^2 - \eta_{\mathbf{x}}^2}} \displaystyle\sum_{n=0}^{N} \sum_{m=0}^{n} \frac{\varepsilon_m}{\Lambda_{mn}} je_{mn}(q, \xi_{\mathbf{s}}) he'_{mn}(q, \xi_{\mathbf{x}}) \\ \qquad S_{mn}(q, \eta_{\mathbf{s}}) S_{mn}(q, \eta_{\mathbf{x}}) \cos[m(\phi_{\mathbf{s}} - \phi_{\mathbf{x}})], \ \xi_{\mathbf{x}} > \xi_{\mathbf{s}}, \\ L_N^I(\mathbf{s}, \mathbf{x}) = -2ik \dfrac{\sqrt{\xi_{\mathbf{x}}^2 - 1}}{c\sqrt{\xi_{\mathbf{x}}^2 - \eta_{\mathbf{x}}^2}} \displaystyle\sum_{n=0}^{N} \sum_{m=0}^{n} \frac{\varepsilon_m}{\Lambda_{mn}} je'_{mn}(q, \xi_{\mathbf{x}}) he_{mn}(q, \xi_{\mathbf{s}}) \\ \qquad S_{mn}(q, \eta_{\mathbf{s}}) S_{mn}(q, \eta_{\mathbf{x}}) \cos[m(\phi_{\mathbf{s}} - \phi_{\mathbf{x}})], \ \xi_{\mathbf{x}} < \xi_{\mathbf{s}}, \end{cases} \tag{21}$$

$$M^d(\mathbf{s}, \mathbf{x}) = \begin{cases} M_N^E(\mathbf{s}, \mathbf{x}) = -2ik \dfrac{\sqrt{(\xi_{\mathbf{s}}^2 - 1)(\xi_{\mathbf{x}}^2 - 1)}}{c^2\sqrt{(\xi_{\mathbf{s}}^2 - \eta_{\mathbf{s}}^2)(\xi_{\mathbf{x}}^2 - \eta_{\mathbf{x}}^2)}} \displaystyle\sum_{n=0}^{N} \sum_{m=0}^{n} \frac{\varepsilon_m}{\Lambda_{mn}} je'_{mn}(q, \xi_{\mathbf{s}}) he'_{mn}(q, \xi_{\mathbf{x}}) \\ \qquad S_{mn}(q, \eta_{\mathbf{s}}) S_{mn}(q, \eta_{\mathbf{x}}) \cos[m(\phi_{\mathbf{s}} - \phi_{\mathbf{x}})], \ \xi_{\mathbf{x}} \geq \xi_{\mathbf{s}}, \\ M_N^I(\mathbf{s}, \mathbf{x}) = -2ik \dfrac{\sqrt{(\xi_{\mathbf{s}}^2 - 1)(\xi_{\mathbf{x}}^2 - 1)}}{c^2\sqrt{(\xi_{\mathbf{s}}^2 - \eta_{\mathbf{s}}^2)(\xi_{\mathbf{x}}^2 - \eta_{\mathbf{x}}^2)}} \displaystyle\sum_{n=0}^{N} \sum_{m=0}^{n} \frac{\varepsilon_m}{\Lambda_{mn}} je'_{mn}(q, \xi_{\mathbf{x}}) he'_{mn}(q, \xi_{\mathbf{s}}) \\ \qquad S_{mn}(q, \eta_{\mathbf{s}}) S_{mn}(q, \eta_{\mathbf{x}}) \cos[m(\phi_{\mathbf{s}} - \phi_{\mathbf{x}})], \ \xi_{\mathbf{x}} < \xi_{\mathbf{s}} \end{cases} \tag{22}$$

where ε_m is the Neumann factor

$$\varepsilon_m = \begin{cases} 1, & m = 0, \\ 2, & m = 1, \ 2, \ \ldots, \ \infty, \end{cases} \tag{23}$$

and he_{mn} is the radial prolate spheroidal wave function of the third kind and is defined as

$$he_{mn}(q, \xi) = je_{mn}(q, \xi) + i\, ye_{mn}(q, \xi), \tag{24}$$

in which je_{mn} and ye_{mn} are the radial prolate spheroidal wave functions of the first and second kind, respectively, S_{mn} is the angular prolate spheroidal wave function, Λ_{mn} is the normalized constant of the angular prolate spheroidal wave function as shown below [25]:

$$\Lambda_{mn} = \int_{-1}^{1} S_{mn}(q, \eta) S_{mn}(q, \eta) d\eta = 2 \sum_{j=0,1}^{\infty}{}' \frac{(j + 2m)! \left[d_j^{mn}(q)\right]^2}{(2j + 2m + 1) j!} \tag{25}$$

where $d_j^{mn}(q)$ is the expansion coefficient of the angular prolate spheroidal wave functions [25] and $q = ck$. For the detail information of $d_j^{mn}(q)$, it is given in the Appendix. It is noted that U^d and M^d kernels in Eqs. (19) and (22) contain the equal sign of $\xi_{\mathbf{x}} = \xi_{\mathbf{s}}$ while T^d and L^d kernels do not include the equal sign due to the discontinuity across the boundary. For the representations of degenerate kernels, we consult those of Morse and Feshbach [27].

3.2 Expansion for boundary densities

The orthogonal relation of the angular prolate spheroidal wave functions [25] is shown below:

$$\int_{-1}^{1} S_{mn}(q,\eta)S_{mn'}(q,\eta)d\eta, = \begin{cases} \Lambda_{mn}, & n'=n, \\ 0, & n'\neq n. \end{cases} \tag{26}$$

In order to fully utilize the orthogonal relations of the angular prolate spheroidal wave functions, we apply the angular prolate spheroidal wave functions and the triangular function to approximate the acoustic pressure $u(\mathbf{s})$ and its normal derivative $t(\mathbf{s})$ on the spheroidal surface as follows:

$$u(\mathbf{s}) = \sum_{v=0}^{\infty}\sum_{w=0}^{v} g_{wv}S_{wv}(q,\eta_{\mathbf{s}})\cos(w\phi_{\mathbf{s}}) + \sum_{v=1}^{\infty}\sum_{w=1}^{v} h_{wv}S_{wv}(q,\eta_{\mathbf{s}})\sin(w\phi_{\mathbf{s}}), \quad \mathbf{s}\in S, \tag{27}$$

$$t(\mathbf{s}) = \frac{\sqrt{\xi_{\mathbf{s}}^2-1}}{c\sqrt{\xi_{\mathbf{s}}^2-\eta_{\mathbf{s}}^2}}\left[\sum_{v=0}^{\infty}\sum_{w=0}^{v} p_{wv}S_{wv}(q,\eta_{\mathbf{s}})\cos(w\phi_{\mathbf{s}}) + \sum_{v=1}^{\infty}\sum_{w=1}^{v} q_{wv}S_{wv}(q,\eta_{\mathbf{s}})\sin(w\phi_{\mathbf{s}})\right], \quad \mathbf{s}\in S, \tag{28}$$

respectively, where g_{wv}, h_{wv}, p_{wv} and q_{wv} are the unknown coefficients of the boundary densities.

4 Analytical derivation of eigenequations for a confocal prolate spheroidal resonator

Following successful experiences in the annular cases [18,19] and the confocal elliptical case [9], it has been revealed that the corresponding mechanism of the spurious eigensolutions of eigenproblems containing a multiply connected domain depends on the geometry of the inner boundary and the integral formulations. In this paper, we extend to the case of a confocal prolate spheroidal resonator as shown in Fig. 1. The radial parameters of the confocal prolate spheroidal resonator are $\xi=\xi_0$ and $\xi=\xi_1$ for the outer and inner surfaces, respectively. First, we consider the confocal prolate spheroidal resonator subject to the Dirichlet–Dirichlet B.C. as shown below:

$$u(\mathbf{x}) = 0, \ \mathbf{x}\in S_0\cup S_1. \tag{29}$$

Equations (13) and (14) are rewritten as

$$0 = \sum_{j=0}^{1}\int_{S_j} T^d(\mathbf{s}_j,\mathbf{x})u_j(\mathbf{s}_j)dS(\mathbf{s}_j) - \sum_{j=0}^{1}\int_{S_j} U^d(\mathbf{s}_j,\mathbf{x})t_j(\mathbf{s}_j)dS(\mathbf{s}_j), \ \mathbf{x}\in V^c\ \cup\ S, \tag{30}$$

$$0 = \sum_{j=0}^{1}\int_{S_j} M^d(\mathbf{s}_j,\mathbf{x})u_j(\mathbf{s}_j)dS(\mathbf{s}_j) - \sum_{j=0}^{1}\int_{S_j} L^d(\mathbf{s}_j,\mathbf{x})t_j(\mathbf{s}_j)dS(\mathbf{s}_j), \ \mathbf{x}\in V^c\ \cup\ S, \tag{31}$$

and boundary flux densities are expressed by

$$t_j(\mathbf{s}_j) = \frac{\sqrt{\xi_j^2-1}}{c\sqrt{\xi_j^2-\eta_{\mathbf{s}_j}^2}}\left[\sum_{v=0}^{\infty}\sum_{w=0}^{v} p_{wv}^{j}S_{wv}(q,\eta_{\mathbf{s}_j})\cos(w\phi_{\mathbf{s}_j}) + \sum_{v=1}^{\infty}\sum_{w=1}^{v} q_{wv}^{j}S_{wv}(q,\eta_{\mathbf{s}_j})\sin(w\phi_{\mathbf{s}_j})\right], \quad \mathbf{s}_j\in S_j \tag{32}$$

where p_{wv}^j and q_{wv}^j are the unknown coefficients of the boundary density on S_j $(j=0,\ 1)$. Substituting Eqs. (19), (20), (29) and (32) to Eq. (30) and collocating the field point exactly on the outer surface S_0, we have

$$\begin{aligned} 4\pi ikc(\xi_0^2-1)&\left(\sum_{v=0}^{\infty}\sum_{w=0}^{v} je_{wv}(q,\xi_0)he_{wv}(q,\xi_0)S_{wv}(q,\eta_{\mathbf{x}})\cos(w\phi_{\mathbf{x}})p_{wv}^0\right.\\ &\left.+\sum_{v=1}^{\infty}\sum_{w=1}^{v} je_{wv}(q,\xi_0)he_{wv}(q,\xi_0)S_{wv}(q,\eta_{\mathbf{x}})\sin(w\phi_{\mathbf{x}})q_{wv}^0\right)\\ +4\pi ikc(\xi_1^2-1)&\left(\sum_{v=0}^{\infty}\sum_{w=0}^{v} je_{wv}(q,\xi_1)he_{wv}(q,\xi_0)S_{wv}(q,\eta_{\mathbf{x}})\cos(w\phi_{\mathbf{x}})p_{wv}^1\right.\\ &\left.+\sum_{v=1}^{\infty}\sum_{w=1}^{v} je_{wv}(q,\xi_1)he_{wv}(q,\xi_0)S_{wv}(q,\eta_{\mathbf{x}})\sin(w\phi_{\mathbf{x}})q_{wv}^1\right) = 0. \end{aligned} \tag{33}$$

By employing the orthogonal relations for the field point (ξ_1), we have

$$(\xi_0^2-1)je_{mn}(q,\xi_0)he_{mn}(q,\xi_0)p_{mn}^0+(\xi_1^2-1)je_{mn}(q,\xi_1)he_{mn}(q,\xi_0)p_{mn}^1=0, \tag{34}$$

$$(\xi_0^2-1)je_{mn}(q,\xi_0)he_{mn}(q,\xi_0)q_{mn}^0+(\xi_1^2-1)je_{mn}(q,\xi_1)he_{mn}(q,\xi_0)q_{mn}^1=0. \tag{35}$$

By collocating the field point of Eq. (30) exactly on the inner surface S_1, we have

$$\begin{aligned}&4\pi ikc(\xi_0^2-1)\left(\sum_{v=0}^{\infty}\sum_{w=0}^{v}je_{wv}(q,\xi_1)he_{wv}(q,\xi_0)S_{wv}(q,\eta_{\mathbf{x}})\cos(w\phi_{\mathbf{x}})p_{wv}^0\right.\\&\qquad\left.+\sum_{v=1}^{\infty}\sum_{w=1}^{v}je_{wv}(q,\xi_1)he_{wv}(q,\xi_0)S_{wv}(q,\eta_{\mathbf{x}})\sin(w\phi_{\mathbf{x}})q_{wv}^0\right)\\&+4\pi ikc(\xi_1^2-1)\left(\sum_{v=0}^{\infty}\sum_{w=0}^{v}je_{wv}(q,\xi_1)he_{wv}(q,\xi_1)S_{wv}(q,\eta_{\mathbf{x}})\cos(w\phi_{\mathbf{x}})p_{wv}^1\right.\\&\qquad\left.+\sum_{v=1}^{\infty}\sum_{w=1}^{v}je_{wv}(q,\xi_1)he_{wv}(q,\xi_1)S_{wv}(q,\eta_{\mathbf{x}})\sin(w\phi_{\mathbf{x}})q_{wv}^1\right)=0.\end{aligned} \tag{36}$$

By employing the orthogonal relations for the field point (ξ_0), we have

$$(\xi_0^2-1)je_{mn}(q,\xi_1)he_{mn}(q,\xi_0)p_{mn}^0+(\xi_1^2-1)je_{mn}(q,\xi_1)he_{mn}(q,\xi_1)p_{mn}^1=0, \tag{37}$$

$$(\xi_0^2-1)je_{mn}(q,\xi_1)he_{mn}(q,\xi_0)q_{mn}^0+(\xi_1^2-1)je_{mn}(q,\xi_1)he_{mn}(q,\xi_1)q_{mn}^1=0. \tag{38}$$

According to Eqs. (34), (35), (37) and (38), we obtain two simultaneous equations as follows:

$$\begin{bmatrix}(\xi_0^2-1)je_{mn}(q,\xi_0)he_{mn}(q,\xi_0) & (\xi_1^2-1)je_{mn}(q,\xi_1)he_{mn}(q,\xi_0)\\(\xi_0^2-1)je_{mn}(q,\xi_1)he_{mn}(q,\xi_0) & (\xi_1^2-1)je_{mn}(q,\xi_1)he_{mn}(q,\xi_1)\end{bmatrix}\begin{Bmatrix}p_{mn}^0\\p_{mn}^1\end{Bmatrix}=\begin{Bmatrix}0\\0\end{Bmatrix}, \tag{39}$$

$$\begin{bmatrix}(\xi_0^2-1)je_{mn}(q,\xi_0)he_{mn}(q,\xi_0) & (\xi_1^2-1)je_{mn}(q,\xi_1)he_{mn}(q,\xi_0)\\(\xi_0^2-1)je_{mn}(q,\xi_1)he_{mn}(q,\xi_0) & (\xi_1^2-1)je_{mn}(q,\xi_1)he_{mn}(q,\xi_1)\end{bmatrix}\begin{Bmatrix}q_{mn}^0\\q_{mn}^1\end{Bmatrix}=\begin{Bmatrix}0\\0\end{Bmatrix}. \tag{40}$$

In order to obtain a non-trivial solution, the determinant of Eqs. (39) and (40) is equal to zero. For unknown coefficients, $\langle p_{mn}^0\ p_{mn}^1\rangle^T$, we have two possible eigenequations as shown below:

$$je_{mn}(q,\xi_0)ye_{mn}(q,\xi_1)-je_{mn}(q,\xi_1)ye_{mn}(q,\xi_0)=0,\ m=0,1,2,\ldots,n,\ n=0,1,2,\ldots,\infty, \tag{41}$$

$$je_{mn}(q,\xi_1)=0,\ m=0,1,2,\ldots,n,\ n=0,1,2,\ldots,\infty. \tag{42}$$

Similarly, we have two possible eigenequations for unknown coefficients, $\langle q_{mn}^0\ q_{mn}^1\rangle^T$,

$$je_{mn}(q,\xi_0)ye_{mn}(q,\xi_1)-je_{mn}(q,\xi_1)ye_{mn}(q,\xi_0)=0,\ m=1,2,\ldots,n,\ n=1,2,\ldots,\infty, \tag{43}$$

$$je_{mn}(q,\xi_1)=0,\ m=1,2,\ldots,n,\ n=1,2,\ldots,\infty. \tag{44}$$

Although eigenequations can be analytically derived by using only the singular integral formulation, we cannot distinguish whether it is true or spurious. Besides, it is found that eigenvalues are double roots no matter if they are true or spurious eigenvalues, when $m\neq 0$. Based on the hypersingular integral equation of Eq. (31), we also obtain four possible eigenequations. Namely, the following two equations:

$$je'_{mn}(q,\xi_1)=0,\ m=0,1,2,\ldots,n,\ n=0,1,2,\ldots,\infty, \tag{45}$$

$$je'_{mn}(q,\xi_1)=0,\ m=1,2,\ldots,n,\ n=1,2,\ldots,\infty, \tag{46}$$

and the other two are the same like Eqs. (41) and (43). If we employ two different approaches to solve the same problem, we should obtain the same and true solution. Therefore, it indicates that Eqs. (42), (44) and (45), (46) are the spurious eigenequations by using Eqs. (30) and (31), respectively.

Following the above procedures, true and spurious eigenequations for the other three kinds of boundary conditions, namely Neumann–Neumann, Dirichlet–Neumann and Neumann–Dirichlet types, can also be analytically derived. True and spurious eigenequations for problems subject to various boundary conditions (Dirichlet–Dirichlet, Neumann–Neumann, Dirichlet–Neumann and Neumann–Dirichlet) are summarized in Table 1. It is interesting to find that spurious eigenequations depend on the geometry of inner boundary and integral representations. This conclusion agrees well with those of the annular case [18,19] and the confocal elliptical case [9].

5 Numerical examples

In this paper, we focus on the eigenproblem of a confocal prolate spheroidal resonator and consider four kinds of boundary conditions as shown in Fig. 1. The four kinds of boundary conditions are Dirichlet–Dirichlet, Neumann–Neumann, Dirichlet–Neumann and Neumann–Dirichlet types, respectively. The lengths of semi-major and semi-minor axes for the inner prolate spheroid are $a_1 = 1.5$ and $b_1 = 1$, respectively. The radial parameter ξ of the inner prolate spheroid is $\xi_1 = \cosh(\tanh^{-1}(b_1/a_1))$, and the outer prolate spheroid is described by $\xi_0 = 1.5\xi_1$. We list the former ten possible eigenvalues in Tables 2, 3, 4 and 5 including the results of the analytical solutions and those of the FEM. Good agreements are made except the results of spurious eigenvalues because no spurious eigenvalues appear in those of the FEM. Table 6 shows the eigenmodes for the first double roots. It is found that the even mode is symmetric to the plane of $y = 0$, while the odd mode is antisymmetric to the plane of $y = 0$. It is found that the modes on some planes are zero response because those planes are nodal surfaces. Besides, the ABAQUS commercial software has its own post processing, so we plot these eigenmodes obtained by the ABAQUS program in terms of the shading mode.

6 Conclusions

In this paper, we have successfully employed the null-field BIEM in conjunction with degenerate kernels to solve 3D eigenproblems of a confocal prolate spheroidal resonator. The closed-form kernel functions were expanded into degenerate kernels in the prolate spheroidal coordinates. We used angular prolate spheroidal wave functions and triangular functions to expand the boundary densities. In this way, the boundary integral of the prolate spheroidal surface can be exactly determined, and eigenequations can be analytically derived. Based on the results of analytical derivation, it is also revealed that spurious eigensolutions depend on the geometry of the inner boundary and the integral representations. Besides, owing to the symmetry of a confocal prolate spheroid, true and spurious eigenvalues are double roots for $m \neq 0$. Finally, solutions obtained by using the null-field BIEM agree well with those results provided by the commercial finite-element software ABAQUS. Based on the successful experience of this paper, we can attempt to extend the confocal prolate case to the confocal oblate case in the future work. Furthermore, eigenproblems of non-confocal cases can be dealt with in a semi-analytical manner by introducing the adaptive observer system. Although the proposed approach is not suitable for any geometry, the numerical results obtained by the proposed approach are more accurate than those by the conventional BEM. Besides, it is not trivial to analytically study the occurring mechanism of spurious eigenvalues in using BEM or BIEM. For the problem with special geometry such as sphere and prolate spheroid, the proposed approach can also analytically solve the problem. Although the degenerate kernel looks more complicated than the closed-form fundamental solution, the main advantage has three aspects. One is analytical integration for singular and hypersingular integrals free of $C.P.V.$ and $H.P.V.$ Another is analytical prediction for the true and spurious eigenvalues. The other is that the BIE is nothing more than the linear algebra after using a degenerate kernel for the BIE.

Table 1 True and spurious eigenequations for the confocal prolate spheroidal resonator subject to various boundary conditions

Figure sketch		Dirichlet–Dirichlet	Neumann–Neumann	Dirichlet–Neumann	Neumann–Dirichlet
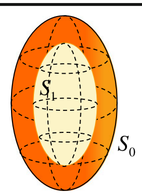		$u(\mathbf{x})=0,\ \mathbf{x}\in S_0$ $u(\mathbf{x})=0,\ \mathbf{x}\in S_1$	$t(\mathbf{x})=0,\ \mathbf{x}\in S_0$ $t(\mathbf{x})=0,\ \mathbf{x}\in S_1$	$u(\mathbf{x})=0,\ \mathbf{x}\in S_0$ $t(\mathbf{x})=0,\ \mathbf{x}\in S_1$	$t(\mathbf{x})=0,\ \mathbf{x}\in S_0$ $u(\mathbf{x})=0,\ \mathbf{x}\in S_1$
Singular formulation	True eigenequation	$je_{mn}(q,\xi_0)ye_{mn}(q,\xi_1)$ $-je_{mn}(q,\xi_1)ye_{mn}(q,\xi_0)=0$	$je'_{mn}(q,\xi_0)ye'_{mn}(q,\xi_1)$ $-je'_{mn}(q,\xi_1)ye'_{mn}(q,\xi_0)=0$	$je_{mn}(q,\xi_0)ye'_{mn}(q,\xi_1)$ $-je'_{mn}(q,\xi_1)ye_{mn}(q,\xi_0)=0$	$je'_{mn}(q,\xi_0)ye_{mn}(q,\xi_1)$ $-je_{mn}(q,\xi_1)ye'_{mn}(q,\xi_0)=0$
	Spurious eigenequation	$je_{mn}(q,\xi_1)=0$	$je_{mn}(q,\xi_1)=0$	$je_{mn}(q,\xi_1)=0$	$je_{mn}(q,\xi_1)=0$
Hypersingular formulation	True eigenequation	$je_{mn}(q,\xi_0)ye_{mn}(q,\xi_1)$ $-je_{mn}(q,\xi_1)ye_{mn}(q,\xi_0)=0$	$je'_{mn}(q,\xi_0)ye'_{mn}(q,\xi_1)$ $-je'_{mn}(q,\xi_1)ye'_{mn}(q,\xi_0)=0$	$je_{mn}(q,\xi_0)ye'_{mn}(q,\xi_1)$ $-je'_{mn}(q,\xi_1)ye_{mn}(q,\xi_0)=0$	$je'_{mn}(q,\xi_0)ye_{mn}(q,\xi_1)$ $-je_{mn}(q,\xi_1)ye'_{mn}(q,\xi_0)=0$
	Spurious eigenequation	$je'_{mn}(q,\xi_1)=0$	$je'_{mn}(q,\xi_1)=0$	$je'_{mn}(q,\xi_1)=0$	$je'_{mn}(q,\xi_1)=0$

Table 2 The former ten eigenvalues for a confocal prolate spheroidal resonator subject to the Dirichlet–Dirichlet boundary condition

Dirichlet–Dirichlet	k_1	k_2	k_3	k_4	k_5	k_6	k_7	k_8	k_9	k_{10}
ABAQUS (no. elements = 92,640)	–	3.434	3.517	3.517	–	3.736	3.742	3.742	3.853	3.853
Present method	2.828 $\begin{pmatrix} n=0 \\ m=0 \end{pmatrix}$	3.436 $\begin{pmatrix} n=0 \\ m=0 \end{pmatrix}$	3.518 $\begin{pmatrix} n=1 \\ m=1 \end{pmatrix}$	3.518 $\begin{pmatrix} n=1 \\ m=1 \end{pmatrix}$	3.649 $\begin{pmatrix} n=1 \\ m=0 \end{pmatrix}$	3.738 $\begin{pmatrix} n=1 \\ m=0 \end{pmatrix}$	3.744 $\begin{pmatrix} n=2 \\ m=2 \end{pmatrix}$	3.744 $\begin{pmatrix} n=2 \\ m=2 \end{pmatrix}$	3.854 $\begin{pmatrix} n=2 \\ m=1 \end{pmatrix}$	3.854 $\begin{pmatrix} n=2 \\ m=1 \end{pmatrix}$

Table 3 The former ten eigenvalues for a confocal prolate spheroidal resonator subject to the Neumann–Neumann boundary condition

Neumann–Neumann	k_1	k_2	k_3	k_4	k_5	k_6	k_7	k_8	k_9	k_{10}
ABAQUS (no. elements = 92,640)	0	0.840	0.885	0.885	1.435	1.465	1.465	1.561	1.561	2.010
Present method	0 $\begin{pmatrix} n=0 \\ m=0 \end{pmatrix}$	0.840 $\begin{pmatrix} n=1 \\ m=0 \end{pmatrix}$	0.886 $\begin{pmatrix} n=1 \\ m=1 \end{pmatrix}$	0.886 $\begin{pmatrix} n=1 \\ m=1 \end{pmatrix}$	1.435 $\begin{pmatrix} n=2 \\ m=0 \end{pmatrix}$	1.465 $\begin{pmatrix} n=2 \\ m=1 \end{pmatrix}$	1.465 $\begin{pmatrix} n=2 \\ m=1 \end{pmatrix}$	1.562 $\begin{pmatrix} n=2 \\ m=2 \end{pmatrix}$	1.562 $\begin{pmatrix} n=2 \\ m=2 \end{pmatrix}$	2.010 $\begin{pmatrix} n=3 \\ m=0 \end{pmatrix}$

Table 4 The former ten eigenvalues for a confocal prolate spheroidal resonator subject to the Dirichlet–Neumann boundary condition

Dirichlet–Neumann	k_1	k_2	k_3	k_4	k_5	k_6	k_7	k_8	k_9	k_{10}
ABAQUS (no. elements = 92,640)	2.146	2.335	2.335	2.493	2.764	2.764	2.775	2.775	–	2.854
Present method	2.147 $\begin{pmatrix} n=0 \\ m=0 \end{pmatrix}$	2.336 $\begin{pmatrix} n=1 \\ m=1 \end{pmatrix}$	2.336 $\begin{pmatrix} n=1 \\ m=1 \end{pmatrix}$	2.494 $\begin{pmatrix} n=1 \\ m=0 \end{pmatrix}$	2.765 $\begin{pmatrix} n=2 \\ m=2 \end{pmatrix}$	2.765 $\begin{pmatrix} n=2 \\ m=2 \end{pmatrix}$	2.775 $\begin{pmatrix} n=2 \\ m=1 \end{pmatrix}$	2.775 $\begin{pmatrix} n=2 \\ m=1 \end{pmatrix}$	2.828 $\begin{pmatrix} n=0 \\ m=0 \end{pmatrix}$	2.854 $\begin{pmatrix} n=2 \\ m=0 \end{pmatrix}$

Table 5 The former ten eigenvalues for a confocal prolate spheroidal resonator subject to the Neumann–Dirichlet boundary condition

Neumann–Dirichlet	k_1	k_2	k_3	k_4	k_5	k_6	k_7	k_8	k_9	k_{10}
ABAQUS (no. elements = 92,640)	1.376	1.573	1.573	1.642	1.950	1.950	1.957	1.957	1.969	2.368
Present method	1.377 $\begin{pmatrix} n=0 \\ m=0 \end{pmatrix}$	1.574 $\begin{pmatrix} n=1 \\ m=1 \end{pmatrix}$	1.574 $\begin{pmatrix} n=1 \\ m=1 \end{pmatrix}$	1.642 $\begin{pmatrix} n=1 \\ m=0 \end{pmatrix}$	1.950 $\begin{pmatrix} n=2 \\ m=1 \end{pmatrix}$	1.950 $\begin{pmatrix} n=2 \\ m=1 \end{pmatrix}$	1.958 $\begin{pmatrix} n=2 \\ m=2 \end{pmatrix}$	1.958 $\begin{pmatrix} n=2 \\ m=2 \end{pmatrix}$	1.969 $\begin{pmatrix} n=2 \\ m=0 \end{pmatrix}$	2.368 $\begin{pmatrix} n=3 \\ m=0 \end{pmatrix}$

Table 6 The corresponding eigenmodes to the first double roots

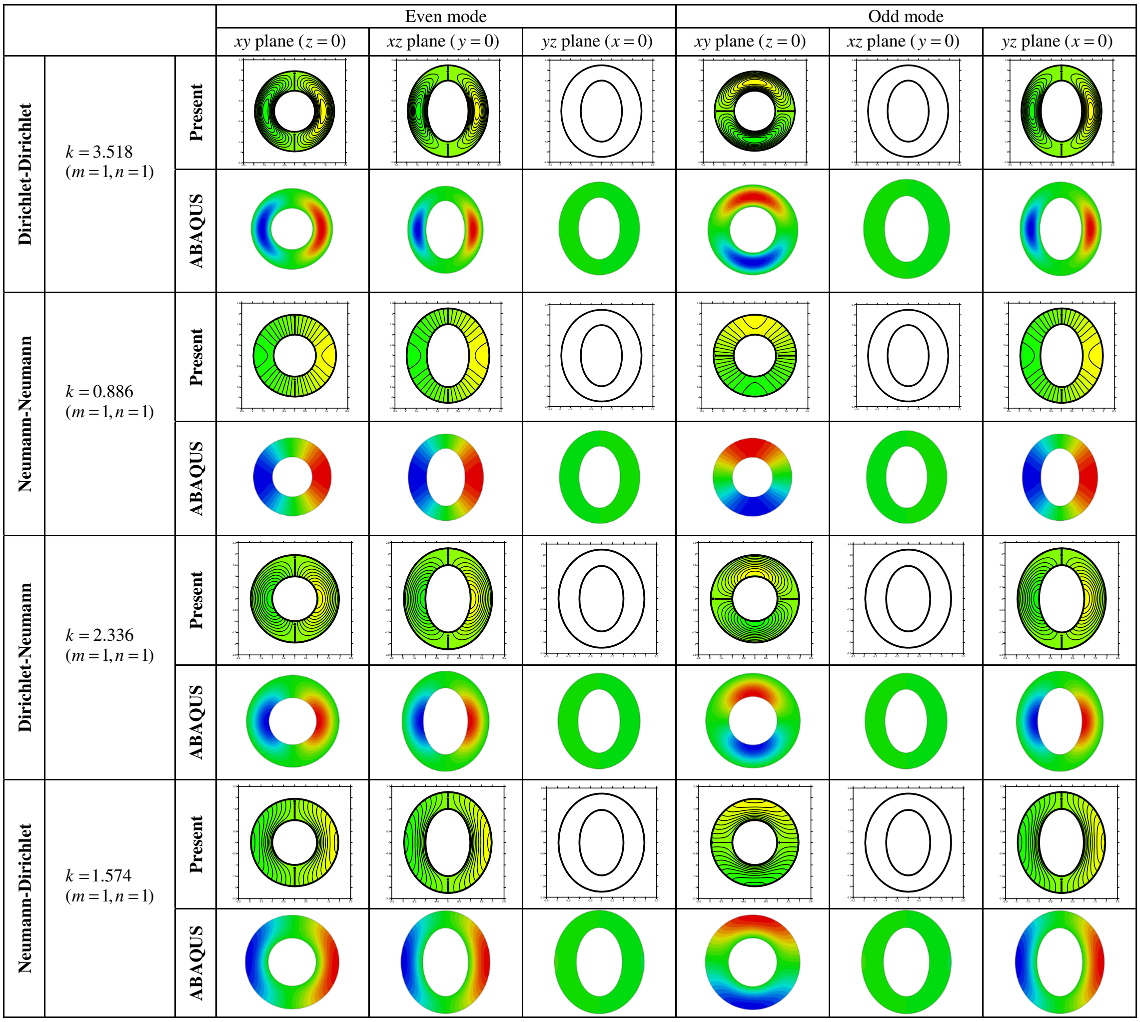

Acknowledgments Financial support from the National Science Council under Grant No. 102-2815-C-019-022-E and NSC99-2221-E-019-015-MY3 for National Taiwan Ocean University is gratefully acknowledged.

Appendix

The normalized constant of the angular prolate spheroidal wave function, Λ_{mn}, can be analytically determined by the following equation [25]:

$$\Lambda_{mn} = \int_{-1}^{1} S_{mn}(q, \eta) S_{mn}(q, \eta) d\eta = 2 \sum_{j=0,1}^{\infty}{}' \frac{(j + 2m)! \left[d_j^{mn}(q)\right]^2}{(2j + 2m + 1) j!} \tag{A1}$$

where $d_j^{mn}(q)$ are the expansion coefficients of the angular prolate spheroidal wave functions, S_{mn}, as shown below:

$$S_{mn}(q, \eta) = \sum_{j=0,1}^{\infty}{}' d_j^{mn}(q) P_{m+j}^{m}(\eta), \tag{A2}$$

in which $P_{m+j}^{m}(\eta)$ is the associated Legendre function of the first kind. The expansion coefficients can be obtained by the following linear eigenvalue equations:

$$\begin{bmatrix} \beta_0 & \alpha_0 & & & & \\ \gamma_2 & \beta_2 & \alpha_2 & & & \\ & & \ddots & & & \\ & & \gamma_{2j} & \beta_{2j} & \alpha_{2j} & \\ & & & & \ddots & \end{bmatrix} \begin{bmatrix} d_0^{mn}(q) \\ d_2^{mn}(q) \\ \vdots \\ d_{2j}^{mn}(q) \\ \vdots \end{bmatrix} = \lambda_{mn}(q) \begin{bmatrix} d_0^{mn}(q) \\ d_2^{mn}(q) \\ \vdots \\ d_{2j}^{mn}(q) \\ \vdots \end{bmatrix}, \quad (n-m = \text{even}), \tag{A3}$$

$$\begin{bmatrix} \beta_1 & \alpha_1 & & & & \\ \gamma_3 & \beta_3 & \alpha_3 & & & \\ & & \ddots & & & \\ & & \gamma_{2j+1} & \beta_{2j+1} & \alpha_{2j+1} & \\ & & & & \ddots & \end{bmatrix} \begin{bmatrix} d_1^{mn}(q) \\ d_3^{mn}(q) \\ \vdots \\ d_{2j+1}^{mn}(q) \\ \vdots \end{bmatrix} = \lambda_{mn}(q) \begin{bmatrix} d_1^{mn}(q) \\ d_3^{mn}(q) \\ \vdots \\ d_{2j+1}^{mn}(q) \\ \vdots \end{bmatrix}, \quad (n-m = \text{odd}) \tag{A4}$$

where $\lambda_{mn}(q)$ is the characteristic value and

$$\alpha_j = \frac{(2m+j+2)(2m+j+1)}{(2m+2j+5)(2m+2j+3)} q^2, \tag{A5}$$

$$\beta_j = (m+j)(m+j+1) + \frac{2(m+j)(m+j+1) - 2m^2 - 1}{(2m+2j-1)(2m+2j+3)} q^2, \tag{A6}$$

$$\gamma_j = \frac{j(j-1)}{(2m+2j-3)(2m+2j-1)} q^2. \tag{A7}$$

To determine the unique coefficients, normalization for the coefficients is introduced as shown below:

$$\sum_{j=0,1}^{\infty}{}' \frac{(-1)^{(j-\delta)/2}(j+2m+\delta)!}{2^j \left(\frac{j-\delta}{2}\right)! \left(\frac{j+2m+\delta}{2}\right)!} d_j^{mn}(q) = \frac{(-1)^{(n-m-\delta)/2}(n+m+\delta)!}{2^{n-m} \left(\frac{n-m-\delta}{2}\right)! \left(\frac{n+m+\delta}{2}\right)!}, \tag{A8}$$

where

$$\delta = \begin{cases} 0, & n-m = \text{even}, \\ 1, & n-m = \text{odd}. \end{cases} \tag{A9}$$

References

1. Tai, G.R.G., Shaw, R.P.: Helmholtz equation eigenvalues and eigenmodes for arbitrary domains. J. Acoust. Soc. Am. **56**, 796–804 (1974)
2. De Mey, G.: Calculation of eigenvalues of the Helmholtz equation by an integral equation. Int. J. Numer. Methods Eng. **10**, 59–66 (1976)
3. De Mey, G.: A simplified integral equation method for the calculation of the eigenvalues of Helmholtz equation. Int. J. Numer. Methods Eng. **11**, 1340–1342 (1977)
4. Hutchinson, J.R., Wong, G.K.K.: The boundary element method for plate vibrations. In: Proceedings of the ASCE Seventh International Conference on Electronic Computation, pp. 297–311 (1979)
5. Hutchinson, J.R.: Boundary method for time-dependent problems. In: Proceedings of the Fifth Engineering Mechanics Division Conference, ASCE, University of Wyoming, Laramie, pp. 136–139 (1984)
6. Yasko, M.: BEM with the real-valued fundamental solutions for the Helmholtz equation. In: Proceedings of the Seventh International Congress of Sound and Vibration, Germany, pp. 2037–2044 (2000)
7. Duran, M., Miguez, M., Nedelec, J.C.: Numerical stability in the calculation of eigenfrequencies using integral equations. J. Comput. Appl. Math. **130**, 323–336 (2001)
8. Chen, J.T., Chen, C.T., Chen, I.L.: Null-field integral equation approach for eigenproblems with circular boundaries. J. Comput. Acoust. **15**, 401–428 (2007)

9. Chen, J.T., Lee, J.W., Leu, S.Y.: Analytical investigation for spurious eigensolutions of multiply-connected membranes containing elliptical boundaries using the dual BIEM. Int. J. Solids Struct. **48**, 729–744 (2011)
10. Tsai, C.C., Young, D.L., Chen, C.W., Fan, C.M.: The method of fundamental solutions for eigenproblems in domain with and without interior holes. Proc. R. Soc. A **462**, 1433–1466 (2006)
11. Chen, J.T., Kao, S.K., Lee, Y.T.: On the spurious eigenvalues for a concentric sphere in BIEM. Appl. Acoust. **71**, 181–190 (2010)
12. Chang, C.T.M.: Natural resonant frequency of a prolate acoustical resonator. J. Acoust. Soc. Am. **49**, 611–614 (1971)
13. Chen, P.T.: Variational formulation of interior cavity frequencies for spheroidal bodies. J. Acoust. Soc. Am **100**, 2980–2988 (1996)
14. Filippi, P.J.T.: Layer potential and acoustic diffraction. J. Sound Vib. **54**, 473–500 (1977)
15. Kokkorakis, G.C., Roumeliotis, J.A.: Acoustic eigenfrequencies in a spheroidal cavity with a concentric penetrable sphere. J. Acoust. Soc. Am **105**, 1539–1547 (1999)
16. Kuo, S.R., Chen, J.T., Huang, C.X.: Analytical study and numerical experiments for true and spurious eigensolutions of a circular cavity using the real-part dual BEM. Int. J. Numer. Methods Eng. **48**, 1401–1422 (2000)
17. Chen, J.T., Lee, J.W., Cheng, Y.C.: On the spurious eigensolutions for the real-part boundary element method. Eng. Anal. Bound. Elem. **33**, 342–355 (2009)
18. Chen, J.T., Lin, J.H., Kuo, S.R., Chyuan, S.W.: Boundary element analysis for the Helmholtz eigenvalue problems with a multiply-connected domain. Proc. R. Soc. A **457**, 2521–2546 (2001)
19. Chen, J.T., Liu, L.W., Hong, H.K.: Spurious and true eigensolutions of Helmholtz BIEs and BEMs for a multiply-connected problem. Proc. R. Soc. A **459**, 1891–1925 (2003)
20. Chen, J.T., Lin, S.Y., Chen, K.H., Chen, I.L.: Mathematical analysis and numerical study of true and spurious eigenequations for free vibration of plates using real-part BEM. Comput. Mech. **34**, 165–180 (2004)
21. Lee, W.M., Chen, J.T.: Analytical study and numerical experiments of true and spurious eigensolutions of free vibration of circular plates using real-part BIEM. Eng. Anal. Bound. Elem. **32**, 368–387 (2008)
22. Chen, J.T., Lee, J.W., Leu, S.Y.: Analytical and numerical investigation for true and spurious eigensolutions of an elliptical membrane using the real-part dual BEM. Meccanica **47**, 1103–1117 (2012)
23. Shi, J., Chen, W., Wang, C.Y.: Free vibration analysis of arbitrary shaped plates by boundary knot method. Acta Mech. Solida Sin. **22**, 328–336 (2009)
24. Chen, W., Shi, J.S., Chen, L.: Investigation on the spurious eigenvalues of vibration plates by non-dimensional dynamic influence function method. Eng. Anal. Bound. Elem. **33**, 885–889 (2009)
25. Zhang, S., Jin, J.: Computation of Special Functions. Wiley, New York (1996)
26. Abramowitz, M., Stegun, I.A.: Handbook of Mathematical Functions with Formulas, Graphs, and Mathematical Tables. Dover, New York (1964)
27. Morse, P., Feshbach, H.: Method of Theoretical Physics. McGraw-Hill, New York (1953)